

V. Thompson, Y. Krivchenkov, V. Riccardo, Z. Vizvary
and JET-EFDA Contributors

Analysis & Design of the Beryllium Tiles for the JET ITER-like Wall Project

“This document is intended for publication in the open literature. It is made available on the understanding that it may not be further circulated and extracts or references may not be published prior to publication of the original when applicable, or without the consent of the Publications Officer, EFDA, Culham Science Centre, Abingdon, Oxon, OX14 3DB, UK.”

“Enquiries about Copyright and reproduction should be addressed to the Publications Officer, EFDA, Culham Science Centre, Abingdon, Oxon, OX14 3DB, UK.”

Assembly, Installation & Upgrade of the JET-EP Halo Current Sensors System

V. Thompson¹, Y. Krivchenkov¹, V. Riccardo¹, Z. Vizvary²
and JET-EFDA Contributors*

¹UKAEA/Euratom Fusion Association, Culham Science Centre, Abingdon, OX14 3DB, UK.

²BUTE Department of Applied Mechanics, Association EURATOM, H-1111 Budapest,
Muegyetem rkp. 5, Hungary

*See annex of J. Pamela et al, "Overview of JET Results",
(Proc. 12th IAEA Fusion Energy Conference, Vilamoura, Portugal (2004)).

Preprint of Paper to be submitted for publication in Proceedings of the
SOFT Conference,
(Warsaw, Poland 11th – 15th September 2006)

ABSTRACT

Work is in progress to completely replace, in 2008/9, the existing JET CFC tiles with a configuration of plasma facing materials consistent with the ITER design. The ITER-like Wall (ILW) will be created with a combination of beryllium (Be), tungsten (W), W-Coated CFC and Be-Coated inconel tiles, with the material depending on the local anticipated heat flux and geometry. Over 4000 tiles will be replaced and the ILW will accommodate additional heating up to at least 50MW for 10s. One of the objectives is to maintain or improve the existing CFC tile power handling performance which has been achieved in most cases by hiding bolt holes, optimising tile size and profile and introducing castellations on plasma facing surfaces.

This paper describes the generic problems associated with the Be tiles (power handling capacity and disruption induced eddy currents) and illustrates the solution selected for the IWGL (Inner Wall Guard Limiter).

1. INTRODUCTION

Figure 1 shows the current configuration inside the JET torus with CFC tiles. These tiles are inertially cooled, and all the new Be tiles will also be inertially cooled. The Be melting temperature of 1289°C will drive their power handling performance. At 40mm typical thickness, the tiles are “thermally thick” for typical 10s pulses and will handle up to about 60MJ/m² without melting. Surface castellations and kinematic restraints will be used to minimise thermally induced stresses. As the thermal flux arrives along near toroidal directions, the design keeps the exposed depth of poloidally running edges to low levels: down to 40µm in the most severe positions. This limit strongly constrains the dimensions of the castellation grooves and the location of the cuts described below. Shaping of the plasma facing surfaces of the tiles, to optimise power handling, is covered in [1].

During disruptions, Be tiles are subjected to eddy current torques due to the combination of large changes in magnetic field (typically 100T/s), high magnetic fields ($B_\phi \sim 4\text{T}$ in the centre of the plasma) and the low resistivity of Be (0.08µΩm at 200°C, the minimum operating temperature of JET). The ILW Be tiles will manage these torques via a combination of the castellations, along with cuts which will interrupt the eddy current loops. The cuts result in the division of the tiles into several slices which require inconel carrier “toast racks” for support. The tile assembly must also withstand e/m forces due to halo currents which, during disruptions, pass between plasma and vacuum vessel via the tiles.

2. POWER HANDLING.

The power handling of the tiles is driven by the need to (a) avoid surface melting and (b) reduce thermally induced stresses to give an adequate fatigue life. For the typical JET cycle of pulses lasting 10s at 20 minute intervals, the melting limit combined with the thermal conductivity and capacity of Be gives an upper bound to the power handling (q_n measured normal to the tile) of about 6MW/m² and a minimum thickness, d , of about 40mm (see Figure 2). The power level of

6MW/m² would apply in cold start cases where the pre-pulse tile temperature is 200°C. Between pulses, the tiles cool by radiation exchange within the torus and so the tile bulk temperature will rise after a number of pulses to the hot start case of about 400°C. This will reduce the power handling capacity to about 4MW/m².

The fatigue life issue is much more complicated to quantify due to a number of factors. In particular there are only limited data on relevant mechanical properties of Be at elevated temperatures, and so the aim here is to minimise thermally induced stress as far as practical in order to maximise the fatigue life. The thermal stresses depend on the temperature profile and the degree of constraint in the tiles. At the tile level these constraints have been eliminated by using kinematic supports which allow the tile to both expand and bow in response to the thermal expansion. At the local level, castellations have been introduced (see Figure 2) to further relieve the constraints, and these have been sized following an extensive program of coupled thermal and mechanical analyses using FE (Finite Elements) using the ANSYS [2] and ABAQUS [3] codes.

These models capture the transient temperatures and thermally induced stresses in a castellated tile and have been used to explore the sensitivity of thermal stress to the castellation geometry: plan size, p, depth, c, and root detail. Figure 3 shows the results of one study on the effect of castellation depth. The graph plots the variation of stress with distance through the tile (plasma surface to the right) for several castellation depths with a 6mm × 6mm area (p × p). Comparison with the zero depth case shows the benefit of castellations. The low ductility of Be at high temperature could severely limit the fatigue life of an un-castellated tile.

The Coffin relation gives a simple method of assessing low cycle fatigue for strain controlled loading which applies here and where test data are limited:

$$\Delta\epsilon \sqrt{N} = \frac{1}{2} \ln \left(\frac{100}{100-RA} \right) \quad (1)$$

Here $\Delta\epsilon$ is the cyclic strain range, N is the estimated number of cycles to failure and RA is the Reduction in Area (%) of the material in a simple tensile test. In this simple form, applicable to low cycle fatigue, the equation assumes that the strain range is wholly plastic. Table 1 summarises the results of several cases. The un-castellated case is considered to be unacceptable as the ductility of Be reduces with temperature above about 400°C, and indeed is unknown above 600°C. With castellations, the surface cyclic strain is all but eliminated and now the critical point becomes the castellation root. The fatigue life estimate, based on the Coffin relation is 8300-18000 cycles depending on the root profile (RA = 50% at 380°C).

The studies concluded that the optimum castellation size is 6mm × 6mm area x 16mm deep with a keyhole profile as this gave similar thermal and mechanical performance, but for practical reasons the area has been increased to 12mm × 12mm and the keyhole replaced by a half-round in most cases.

3. HOT SPOTS.

The requirement for castellations and slicing of the tiles (to reduce eddy currents as described below) results in small exposed edges on the toroidally facing surfaces as shown in Figure 2. With typical angles of attack, α , to the normal face of 1-5deg, the heat flux on the exposed edges is 45 –230MW/m² and the edge exposure must be minimised to avoid hot spot melting. Detailed FE and analytical models have provided results for sensitivity studies to arrive at design limits for the exposed depths (and the associated toroidal gaps). The analytical solutions, [4], for surface heating of thick plates subjected to a surface flux, q_n (uniform case) or q_ϕ (edge heating over a width of a) are:

$$\Delta T_n = \frac{2q_n}{k} \sqrt{\frac{\kappa t}{\pi}} \quad (2)$$

$$\Delta T_\phi = \frac{q_\phi}{k} \left(\frac{2}{a} \sqrt{\frac{\kappa t}{\pi}} \operatorname{erf} \left(\frac{a}{2\sqrt{\kappa t}} \right) - \frac{1}{\pi} Ei \left(\frac{-a^2}{4\kappa t} \right) \right) \quad (3)$$

Here $\kappa = k/(\rho.C_p)$ where k , ρ and C_p are the Be conductivity, density and specific heat respectively. $Ei(x)$ is the exponential integral function given by:

$$Ei(x) = - \int_{-x}^{\infty} \frac{\exp(-u)}{u} du \quad (4)$$

By adding the two solutions, the corner temperature variation with exposure can be obtained as shown in Figure 4.

As the exposures reduce, the results converge on a temperature of about 840°C (for 4 MW/m²) which is the case for face heating only. Although the change with exposure is fairly small, the proximity to melting means that only small exposures can be tolerated and a value of 40µm has been set to be consistent with the 4 MW/m² and 1 deg case and leave some margin. In consequence, the IWGL tile employs a large block in the central region where the heat flux is high. This block contains only castellations which have small exposures. The slices, which are needed to reduce eddy currents but which cannot be assembled with accuracy sufficient to ensure exposed edges are <40 micron, are banished to the outer regions of the tile where the heat flux is lower and so greater exposures can be tolerated.

4. EDDY CURRENT LOADS AND CHOICE OF SLICING DESIGN.

Plasma disruptions produce large changes in magnetic field, dB/dt , which induce eddy currents in the conducting materials. For CFC tiles, the electrical resistivity is about 10 µ m and eddy currents are small, but for Be tiles the resistivity reduces to 0.08 µ m (at 200 °C) and eddy currents become an issue. The currents interact with the local magnetic field, B , to produce a torque, T , which can be estimated using the analytical solution for a rectangular plate (see Figure 5).

$$T = \sigma \cdot (dB/dt) \cdot t \cdot \left(\frac{w}{2} \cdot \frac{h}{2} \right) \cdot \frac{2^{10}}{\pi^6} \sum_{n=1,3..}^{\infty} \sum_{m=1,3..}^{\infty} \frac{1}{n^3 m^3 \left(\frac{n.h}{m.w} + \frac{n.w}{m.h} \right)} \quad (5)$$

This is the asymptotic solution for fully penetrated eddy currents which is a good approximation here where the typical eddy diffusion time constant (5ms) is smaller than the typical disruption time constant (15ms). The solution is strongly dependent on the plate dimensions w , h and t and is only valid for thin plates ($w, h \gg t$) where t is the thickness out of the current plane.

The ANSYS FE code provides a magnetic solver which gives the eddy torques for general cases. For the ILW project, the plate solution is used where possible since it provides rapid results and a series of test cases have been used to establish its range of validity. The FE analysis is complex as it requires a volume mesh of the conducting part plus a volume mesh around the part to span from the conducting part surface to remote surfaces where the boundary conditions are applied. Figure 6 shows the results of one study which examines the effect of width, w , for tiles with $t = 15$ mm and $h = 100$ mm. The study includes the simple “wire” solution where the current path is assumed to flow along a “picture frame” route and gives the following torque:

$$T = \sigma \cdot (dB/dt) \cdot t \cdot \frac{(w \cdot h)^2}{16 \cdot \left(\frac{w}{h} + \frac{h}{w}\right)} \quad (6)$$

The three methods are in good agreement and illustrate the strong dependence of torque on width. The simplicity of the plate solution has been exploited in more complicated cases by building more complex geometry from a “jig-saw” of rectangles: with the FE method only used where the plate results indicate small margins on torque handling and for spot checks. These cases have shown that the plate solution can under-estimate the torque by up to about 50%.

Calculations for the IWGL clearly show that a full tile (250 mm × 100 mm × 40 mm) would give unacceptable eddy torques and so several slicing options have been assessed. The chosen design, described in detail in Sections 5 and 6, has a large central block with side slices to balance the conflicting eddy current and edge heating issues.

5. IWGL BE TILE DESIGN.

Most of the 16 IWGL beams on JET (Figure 1 shows the current CFC arrangement) will be covered with 19 standard Be tile assemblies and special assemblies at top and bottom. Figure 7 shows an exploded view of a single standard assembly which consists of five Be slices supported on a “toast rack” carrier via six pins. The carrier will be made from inconel, and the support arrangement allows the Be to “breathe” thermally whilst resisting e/m forces via the pins and fins on the carrier. Be and Inconel have similar expansion coefficients, but they are not well coupled thermally and so temperature differences of typically 200°C will occur and this demands suitable expansion clearances.

The carrier and tile assembly will be remotely installed and attached to the IWGL beam by two M10 bolts located above the Be. Assembly will start with the tile at the bottom of the beam; successive tiles will cover the bolts of the tile below. A special top tile covers the last pair of bolts and this arrangement avoids the use of plasma facing holes in the Be which would seriously limit the power handling of the tiles.

The e/m forces include the eddy torques discussed above plus forces due to the interaction of magnetic fields and halo currents carried from the plasma via the tiles into the IWGL beam. Figure 7 shows a typical halo current path which crosses both toroidal and poloidal fields.

6. STRUCTURAL ANALYSIS OF TILE CARRIERS.

The carrier design is driven by its interfaces with the sliced Be, the existing IWGL beam, the requirement for remote handling and the limited space available. The requirements result in the complex geometry shown above, which together with the large number required (>300 for the IWGL alone) means that casting is the appropriate manufacturing route. This limits the choice of suitable materials which has been short-listed to: inconel 600 air-cast, vacuumcast 625 and vacuum-cast 713LC in order of preference based on cost and ease of manufacture. The final choice depends on the strength requirement and the complexity of the geometry and loading means that detailed FE analysis is needed for the assessment.

Figure 8 shows the carrier FE model which was meshed in ANSYS using 10-noded tetrahedral elements on a de-featured CAD model. This figure shows the faces which contact the adjacent carriers, simulated here using periodic boundary conditions. Figure 9 shows the patches on the bottom of the carrier which are in contact with the supporting beam. The contacts with adjacent carriers are needed since the hidden bolting arrangement leaves the carriers vulnerable to disruption e/m forces which, in some cases, tend to lever the tile off the beam. Hence the carriers support one another in the normal direction with tongues and grooves.

Disruption forces arise in the carrier due to eddy torques in the Be slices, eddy torques in the carrier itself and halo current forces. The halo forces are usually calculated analytically by simplifying the anticipated current path to a set of straight-line segments with spot checks made using the ANSYS e/m facility. The ANSYS method requires a volume mesh only of the conducting part here, as the boundary conditions are specified by applying distributed current sources on the faces wetted by the plasma. The eddy and halo forces are applied to the carrier via nodal loads on the carrier fins and pin-hole surfaces. The stresses in the pins and in the Be itself are analysed separately. Bolt pre-loads are first applied and then the e/m loads added with various combinations of eddy and halo considered taking into account (a) the eddy loads may be of either sign and (b) with one load at peak, the other load is a less than 40% of its peak value. This combined load factor is based on existing experience in JET. The frequency content of the e/m loads (< 50Hz) is low compared with the expected natural frequency of the carrier (> 100Hz) and so quasi-static conditions are assumed.

Here the eddy loads dominate and Figure 10 shows the carrier stresses for the “100% eddy + 40% halo” case. The structural integrity of the carrier has been assessed by breaking the stresses down into categories of primary/secondary, membrane/bending/peak and global/local following the methods used in pressure vessel codes e.g. [5]. These results show that the vacuum cast 625 material is suitable. The assessment also examines the attachments and shows that the available bolt pre-load based on a bolt torque of 30Nm is needed to prevent gapping between carrier and beam. However, in order to be sure of being able to remove the bolts for maintenance or decommissioning, a value of 15Nm or

less is preferred based on previous experience in JET. Another factor is that the disruption e/m loads are based on extreme JET conditions (6 MA plasma with 4 T toroidal field on axis) which would impose severe loads on other structures inside JET, so such high level disruptions could only be tolerated for a few pulses at most. As it is unlikely that bolt gapping for only a few pulses would lead directly to bolt failure, a compromise installation torque of 20Nm has been set.

CONCLUSIONS

Complete replacement of the JET CFC tiles with the ITER-like wall tiles in 2008/9 presents many technical challenges. This paper has described the generic challenges associated with the Be tiles which arise mainly as a result of its low melting point and high electrical conductivity. The design meets these challenges and should deliver power handling performance similar to, or better than, the existing CFC tiles. The paper illustrates specific design solutions – hiding bolt holes, plasma surface castellations and tile slicing – for the IWGL tiles.

ACKNOWLEDGEMENTS

This work was funded jointly by the United Kingdom Engineering and Physical Sciences Research Council and by the European Communities under the contract of Association between EURATOM and UKAEA. The views and opinions expressed herein do not necessarily reflect those of the European Commission. This work was carried out within the framework of the European Fusion Development Agreement. The work is complementary to the work on power handling and associated tile surface shaping on the JET ILW Be tiles being presented in a separate paper by I. Nunes et al, [1]. The authors acknowledge that the work presented here involved many members of the ILW team and mention in particular S. de Groot, H. Lachery, T. Ramade and R. Walton.

REFERENCES

- [1]. Power handling of the Beryllium tiles for the ITER-like Wall project at JET, I. Nunes et al., SOFT 2006 - 24th Symposium on Fusion Technology, Warsaw, Poland.
- [2]. Conduction of Heat in Solids. H.S. Carslaw and J.C. Jaeger, Clarendon Press, 2nd Ed. 1959.
- [3]. ANSYS Release 10.0
- [4]. ABAQUS Analysis Users Manual Version 6.6.
- [5]. ASME Boiler and Pressure Vessel Code. Section VIII. Rules for Construction of Pressure Vessels.

Case	$\Delta\epsilon(\text{total})$	Max. Temp.	N Predicted cycles to failure.
Un-castellated surface	0.16%	840°C	Uncertain but low expected
Castellated Surface	<0.01%	840°C	Uncertain but high expected
Castellation root with 0.3mm half round profile	0.38%	380°C	8300
Castellation root with 0.6mm keyhole profile	0.26%	380°C	18000

Table 1: Fatigue assessments for $d = 40\text{mm}$, $q_n = 4\text{ MW/m}^2$ (ave.) for 10sec., $p = 6\text{mm}$ square, $c = 16\text{mm}$, $b = 0.6\text{mm}$. 200°C start temperature

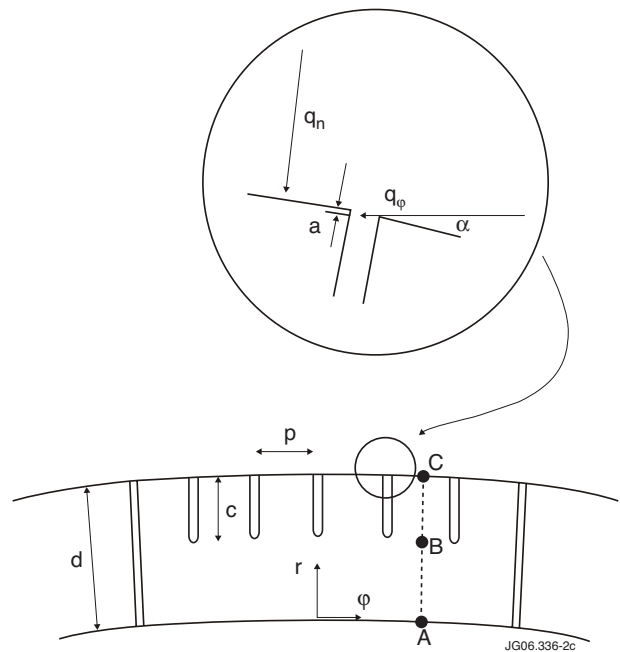
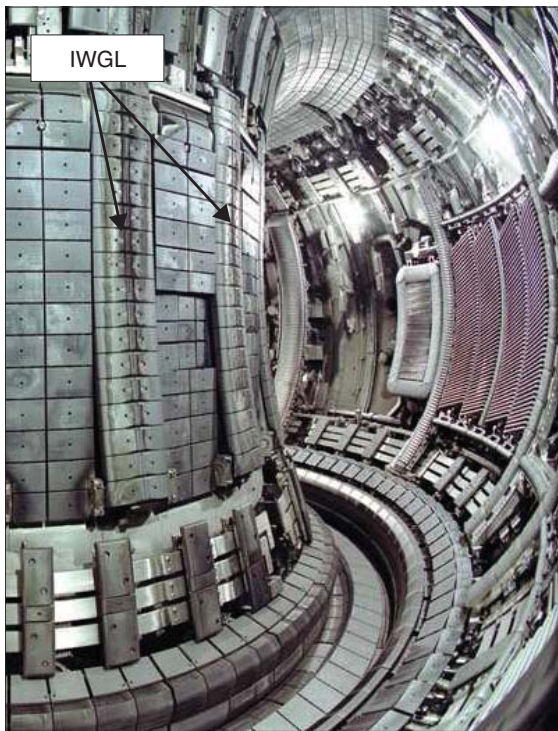


Figure 1: JET showing current configuration with CFC tiles.

Figure 2: Be tile geometry.

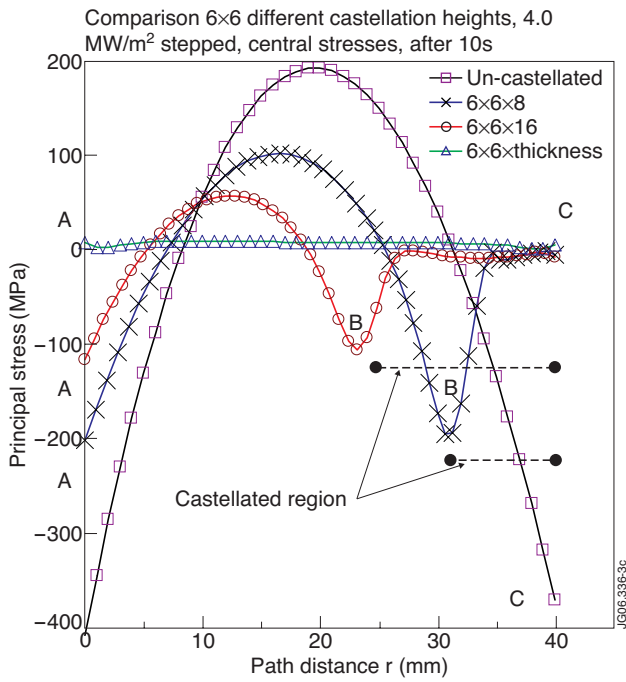


Figure 3: Castellation depth sensitivity study. See Figure 2 for location of points A, B and C. $6 \times 6 \times \text{thickness}$ case illustrates a “full depth” castellation for reference only.

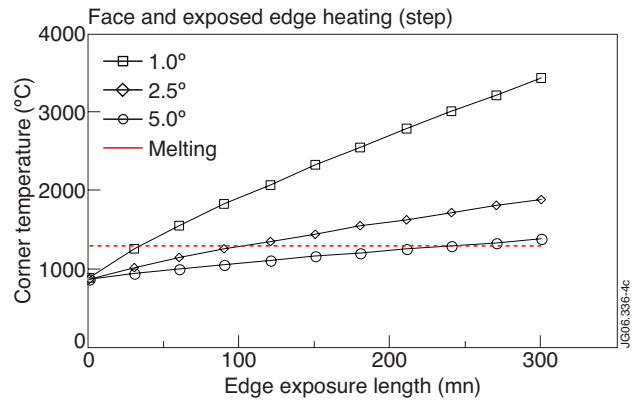


Figure 4: Corner temperature variation with exposure length and angle of attack (α and β in Figure 2). 4 MW/m^2 , 200°C start temperature.

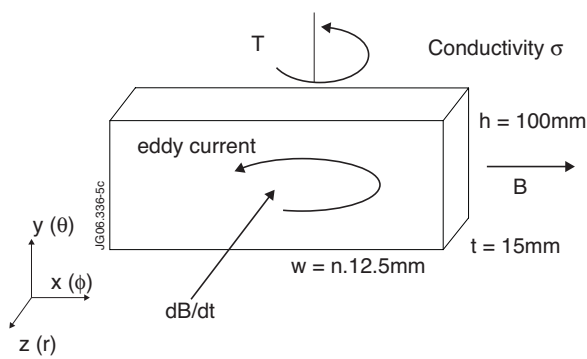


Figure 5: Eddy current geometry.

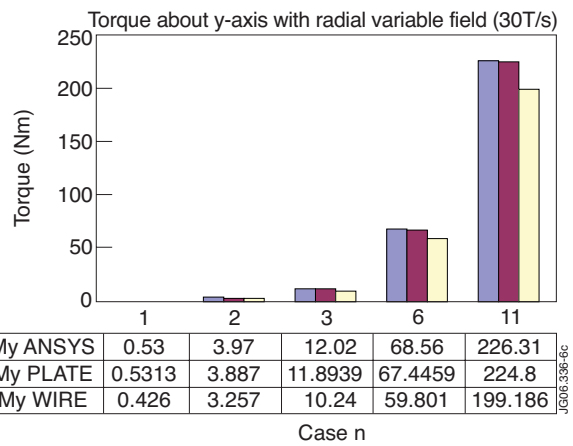


Figure 6: Eddy current torque results.

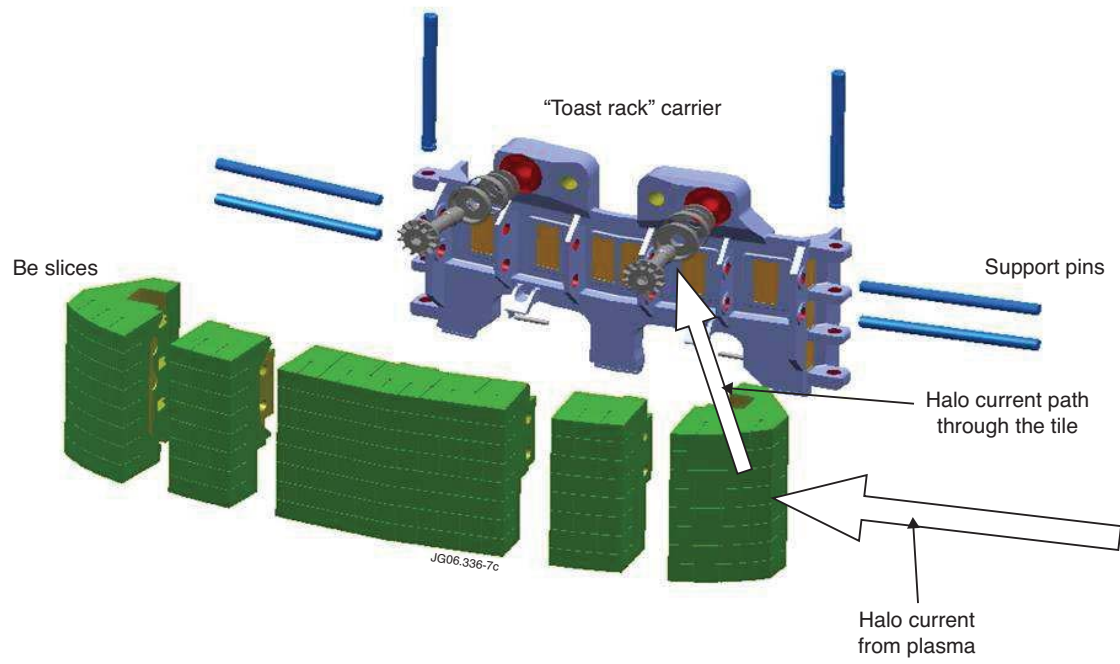


Figure 7: Typical Be IWGL tile assembly. Exploded view.

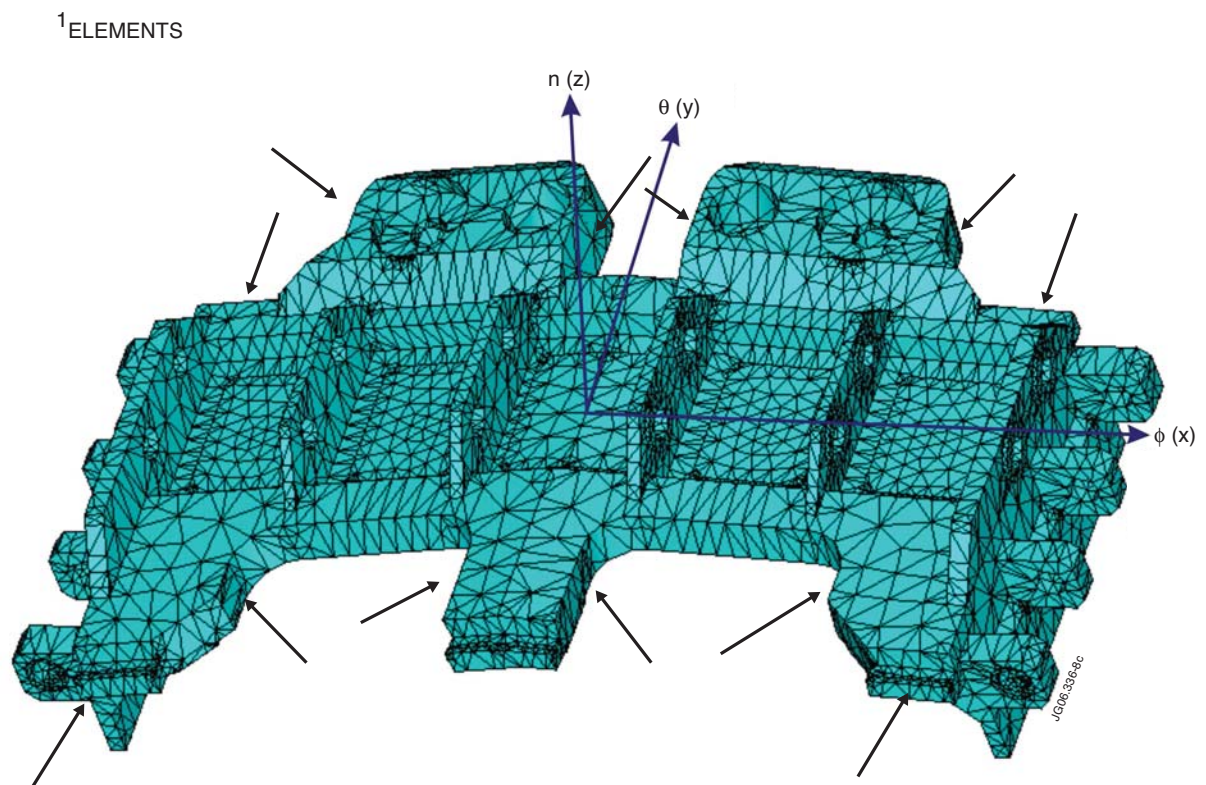


Figure 8: IWGL carrier FE model. Arrows indicate contacts with adjacent carriers.

Elements
Type No.

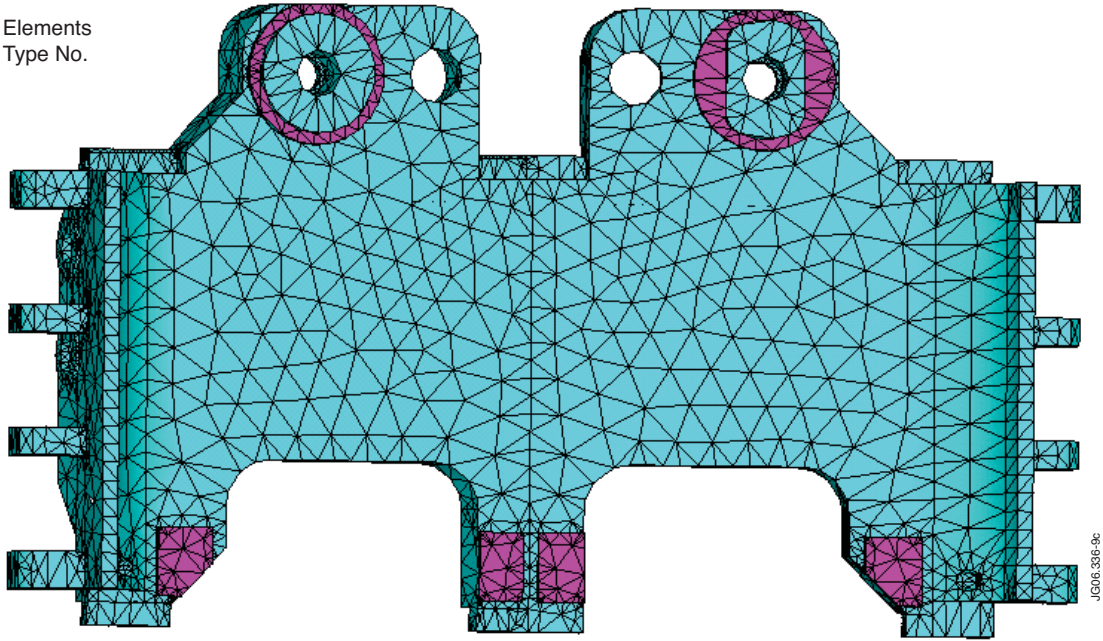


Figure 9: IWGL carrier FE model. Patches indicate contacts to the supporting beam.

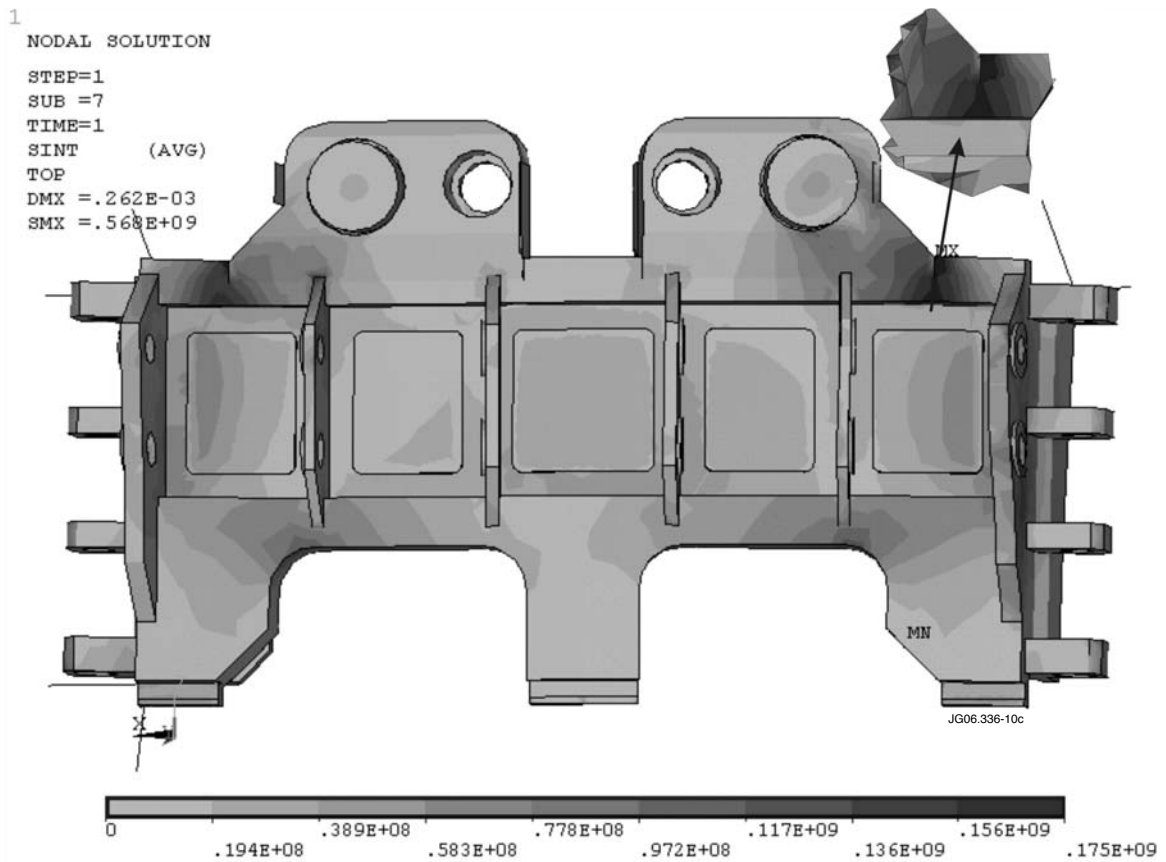


Figure 10: IWGL tile carrier stresses due to disruption forces (Pa).